Electronic Supplementary Material (ESI) for Polymer Chemistry.


# Supporting Information for

## Dispersions of Ultrastable Crown-Ether Functionalized Triphenylamine and Pyrene-Linked Porous Organic Conjugated Polymers with Single-Walled Carbon Nanotube as the High-Performance Electrode for Supercapacitor

**Mohamed Gamal Mohamed,[a,b]* Wan-Chun Chang,[a] Swetha V Chaganti,[c,d] Santosh U Sharma[c,d], Jyh-Tsung Lee,[c,d,e] and Shiao-Wei Kuo[a,e]***

[a]Department of Materials and Optoelectronic Science, Center for Functional Polymers and Supramolecular Materials, National Sun Yat-Sen University, Kaohsiung 804, Taiwan.

[b]Department of Chemistry, Faculty of Science, Assiut University, Assiut 71515, Egypt.

[c]Department of Chemistry, National Sun Yat-Sen University, Kaohsiung, 80424, Taiwan

[I]nternational PhD Program for Science, National Sun Yat-sen University, Kaohsiung 80424, Taiwan

[e]Department of Medicinal and Applied Chemistry, Kaohsiung Medical University, Kaohsiung 807, Taiwan.

**Corresponding authors**:

E-mail: mgamal.eldin12@yahoo.com (M. G. Mohamed) and kuosw@faculty.nsysu.edu.tw (S. W. Kuo).

## Characterization

FTIR spectra were collected on a Bruker Tensor 27 FTIR spectrophotometer with a resolution of 4 $cm^{-1}$ by using the KBr disk method. $^{13}C$ nuclear magnetic resonance (NMR) spectra were examined by using an INOVA 500 instrument with DMSO as the solvent and TMS as the external standard. Chemical shifts are reported in parts per million (ppm). The curing behavior and thermal stabilities of the samples were performed by using a TG Q-50 thermogravimetric analyzer under a $N_2$ atmosphere; the cured sample (ca. 5 mg) was put in a Pt cell with a heating rate of 20 °C $min^{-1}$ from 100 to 800 °C under a $N_2$ flow rate of 60 mL $min^{-1}$. Wide-angle X-ray diffraction (WAXD) patterns were measured by the wiggler beamline BL17A1 of the National Synchrotron Radiation Research Center (NSRRC), Taiwan. A triangular bent Si (111) single crystal was used to get a monochromated beam having a wavelength ($\lambda$) of 1.33 Å. The morphologies of the polymer samples were examined by Field emission scanning electron microscopy (FE-SEM; JEOL JSM7610F) and also by transmission electron microscope (TEM) using a JEOL-2100 instrument at an accelerating voltage of 200 kV. BET surface area and porosimetry measurements of samples (ca. 40–100 mg) were measured using BEL Master™/BEL sim™ (v. 3.0.0). $N_2$ adsorption and desorption isotherms were generated through incremental exposure to ultrahigh-purity $N_2$ (up to ca. 1 atm) in a liquid $N_2$ (77 K) bath. Surface parameters were calculated using BET adsorption models in the instrument's software. The pore size of the prepared samples was determined by using nonlocal density functional theory (NLDFT).

## Electrochemical Analysis

**Working Electrode Cleaning:** Prior to using, the glassy carbon electrode (GCE) was polished several times with 0.05-μm alumina powder, washed with EtOH after each polishing step, cleaned through sonication (5 min) in a water bath, washed with EtOH, and then dried in air.

**Electrochemical Characterization:** The electrochemical experiments were performed in a three-electrode cell using an Autolab potentiostat (PGSTAT204) and 1 M KOH as the aqueous electrolyte. The GCE was

used as the working electrode (diameter: 5.61 mm; 0.2475 $cm^2$); a Pt wire was used as the counter electrode; Hg/HgO (RE-1B, BAS) was the reference electrode. All reported potentials refer to the Hg/HgO potential. A slurry was prepared by dispersing CE-Py POP and CE-Py POP/SWCNT nanocomposite (2 mg), carbon black (2 mg), and Nafion (10 wt%) in a mixture of (EtOH/ $H_2O$) (200 µL: 800 µL) and then sonicating for 1 h. A portion of this slurry (10 µL) was pipetted onto the tip of the electrode, which was then dried in air for 30 min prior to use. The electrochemical performance was studied through CV at various sweep rates (5–200 mV $s^{-1}$) and through the GCD method in the potential range from -1.0 V and 0.0 V (vs. Hg/HgO) at various current densities (0.5–20 A $g^{-1}$) in 1 M KOH as the aqueous electrolyte solution.

The specific capacitance was calculated from the GCD data using the equation.

$$C_s = (I\Delta t)/(m\Delta V)$$

Where $C_s$ (F $g^{-1}$) is the specific capacitance of the supercapacitor, $I$ (A) is the discharge current, $\Delta V$ (V) is the potential window, $\Delta t$ (s) is the discharge time, and $m$ (g) is the mass of the NPC on the electrode. The energy density ($E$, W h $kg^{-1}$) and power density ($P$, W $kg^{-1}$) were calculated using the equations.

$$E = 1000C(\Delta V)^2/(2 \times 3600)$$

$$P = E/(t/3600)$$

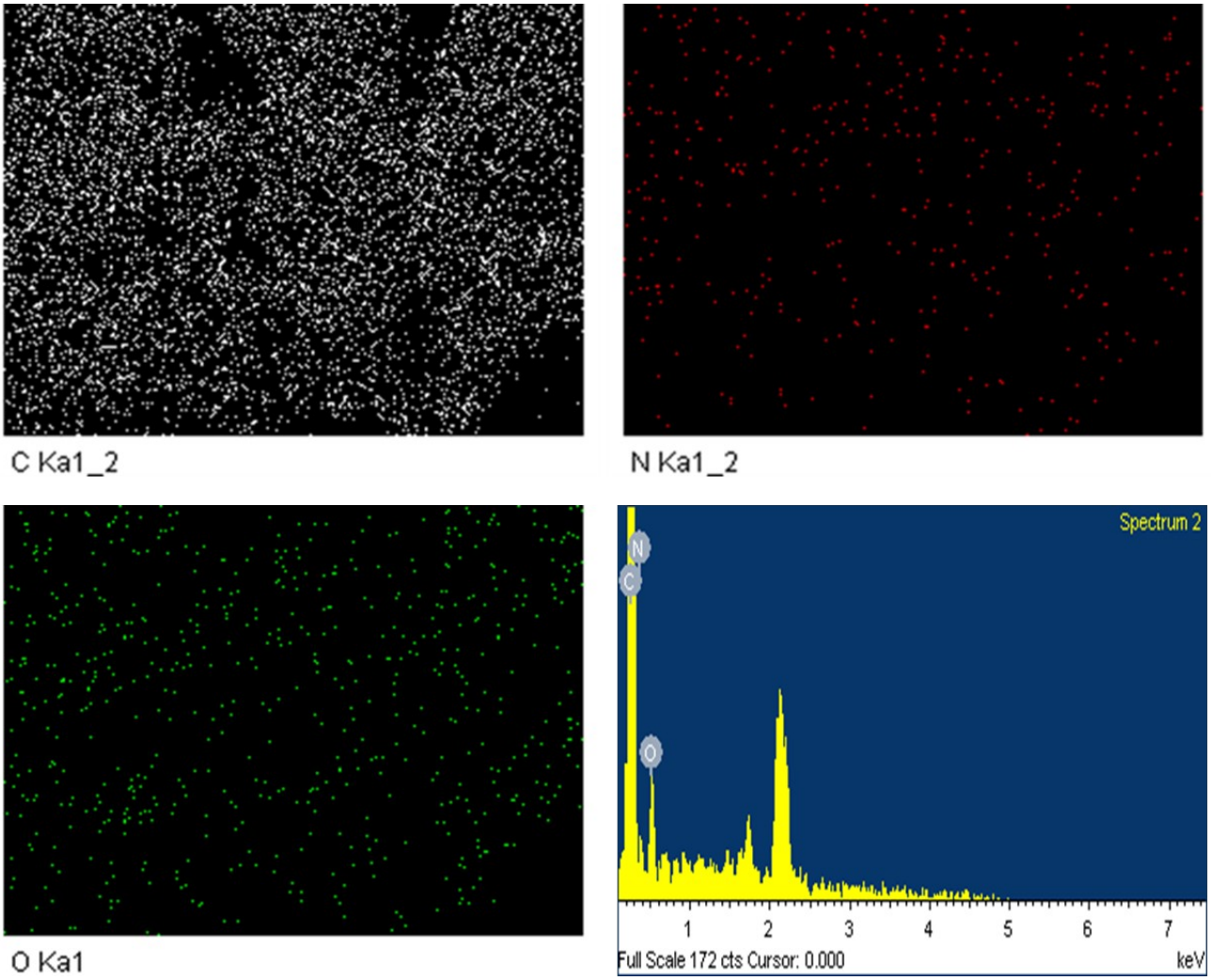


**Figure S1**. SEM-EDS mapping of CE-Py POP.

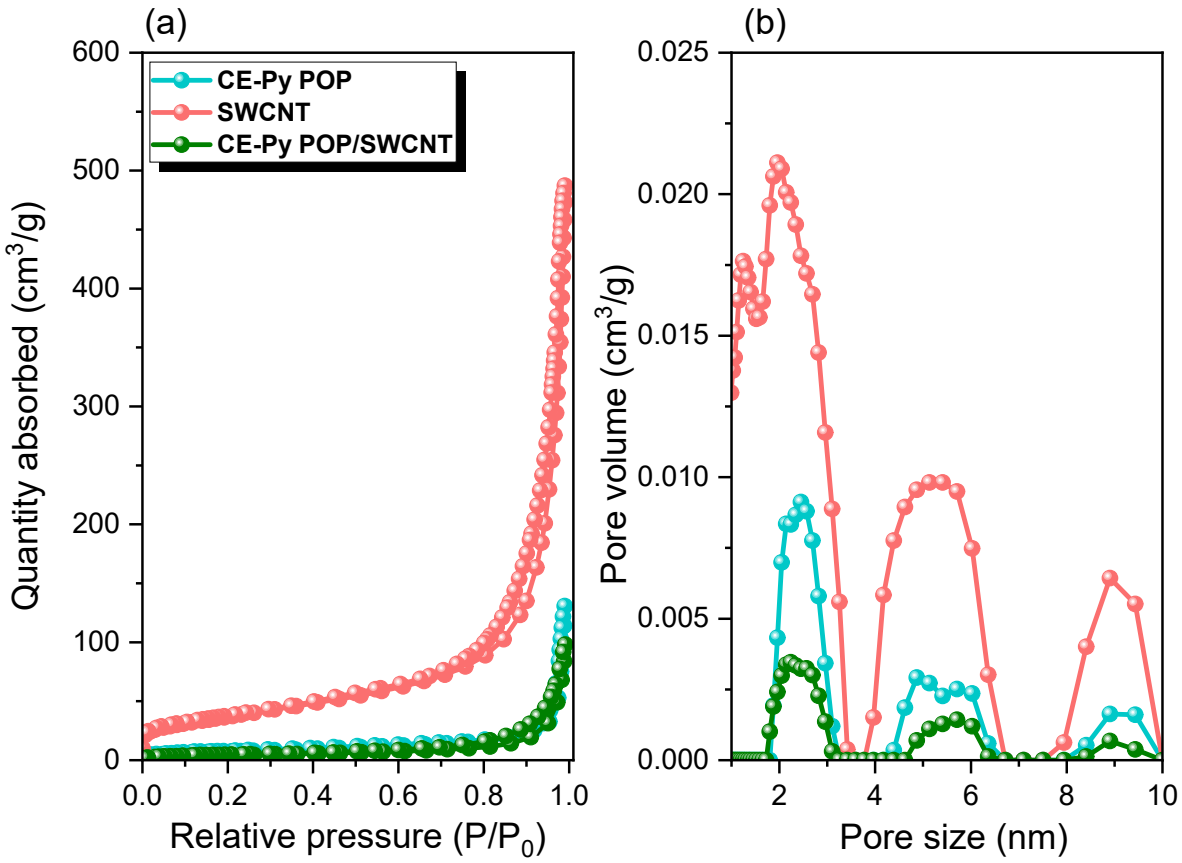


**Figure S2**. (a) $N_2$ adsorption/desorption isotherms, and (b) pore size distributions of CE-Py POP, SWCNT and CE-Py POP/SWCNT.

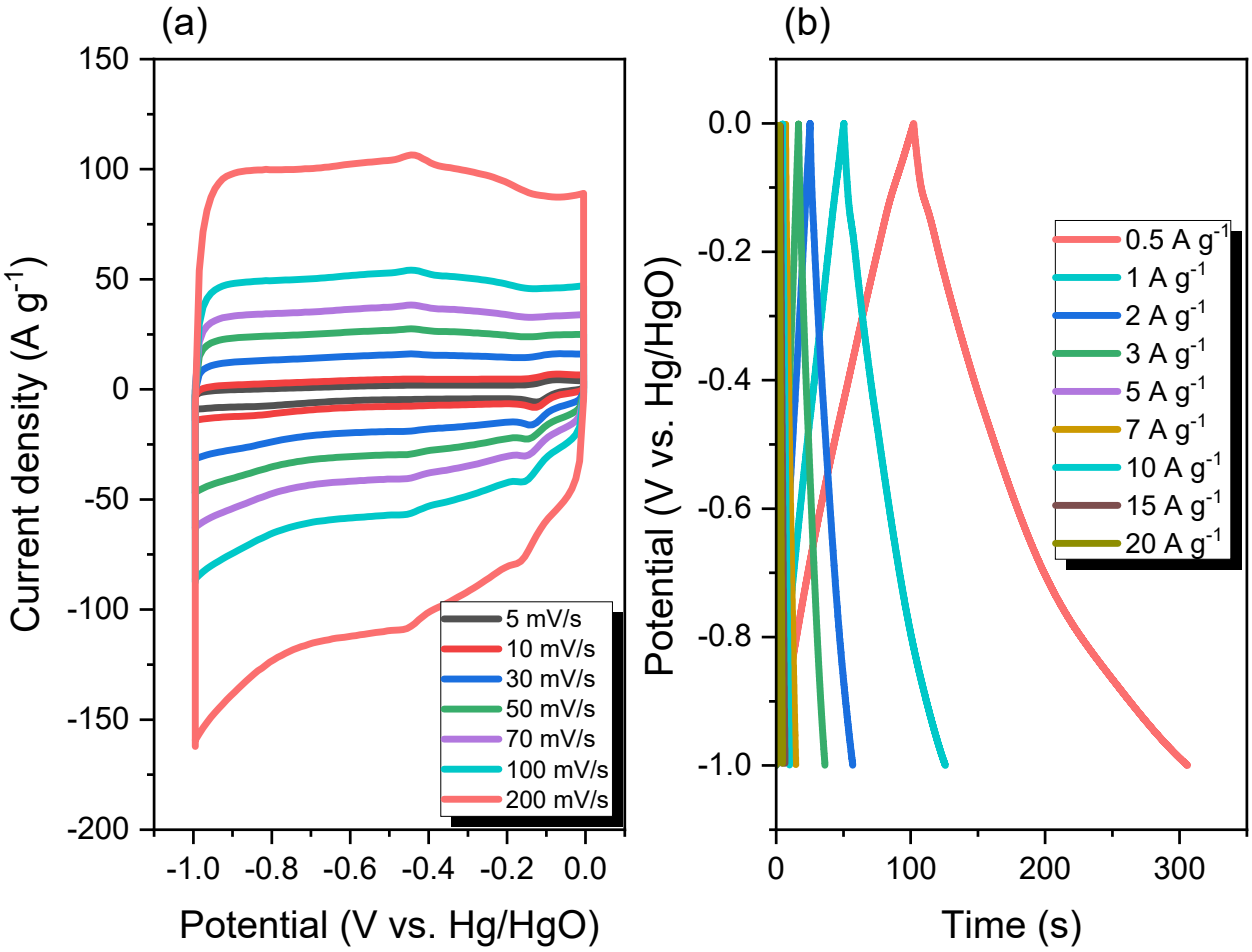


**Figure S3**. (a) CV, and (b) GCD of SWCNT.

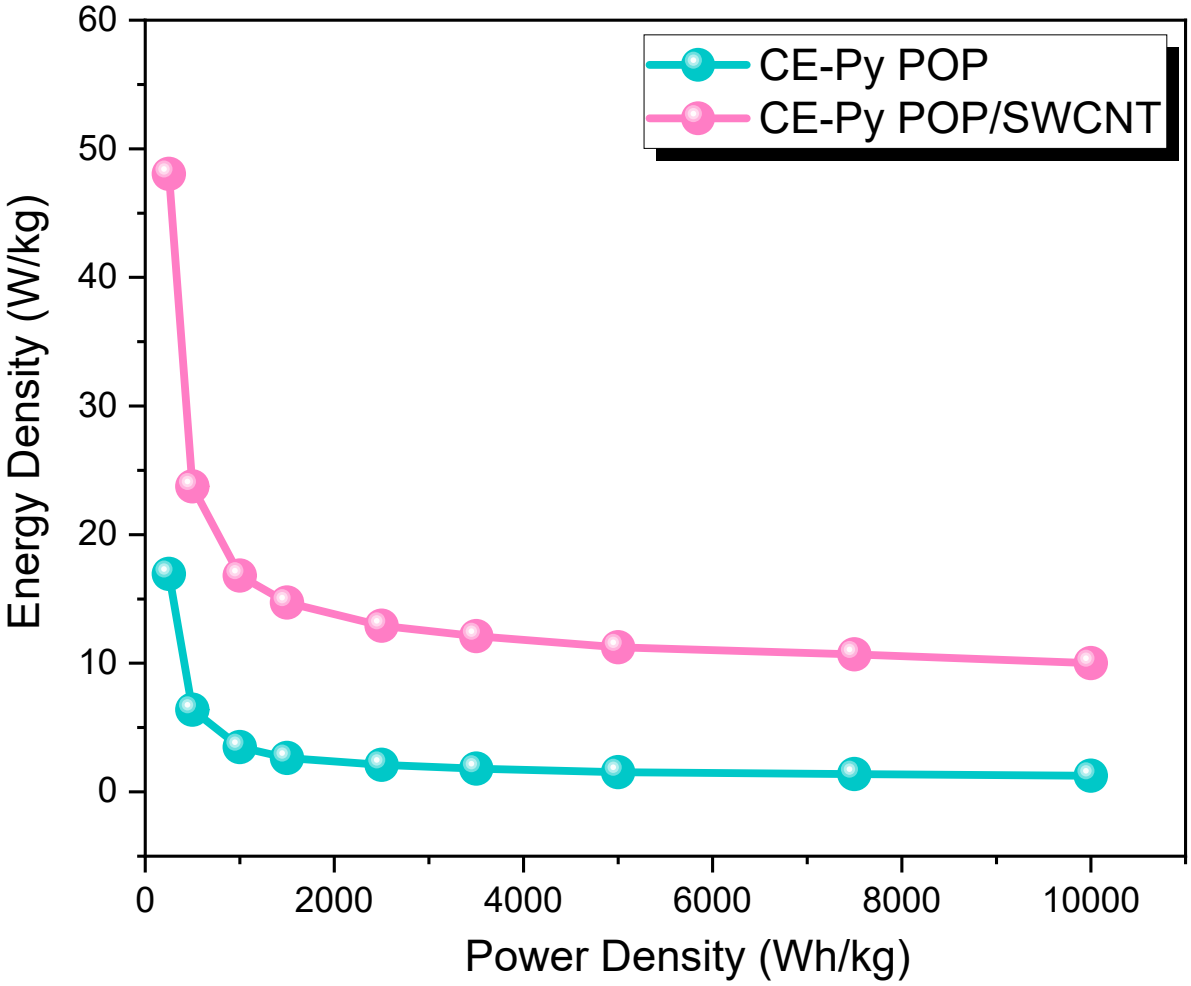


**Figure S4**. Ragone profile of CE-Py POP and CE-Py POP/SWCNT (three electrodes system).

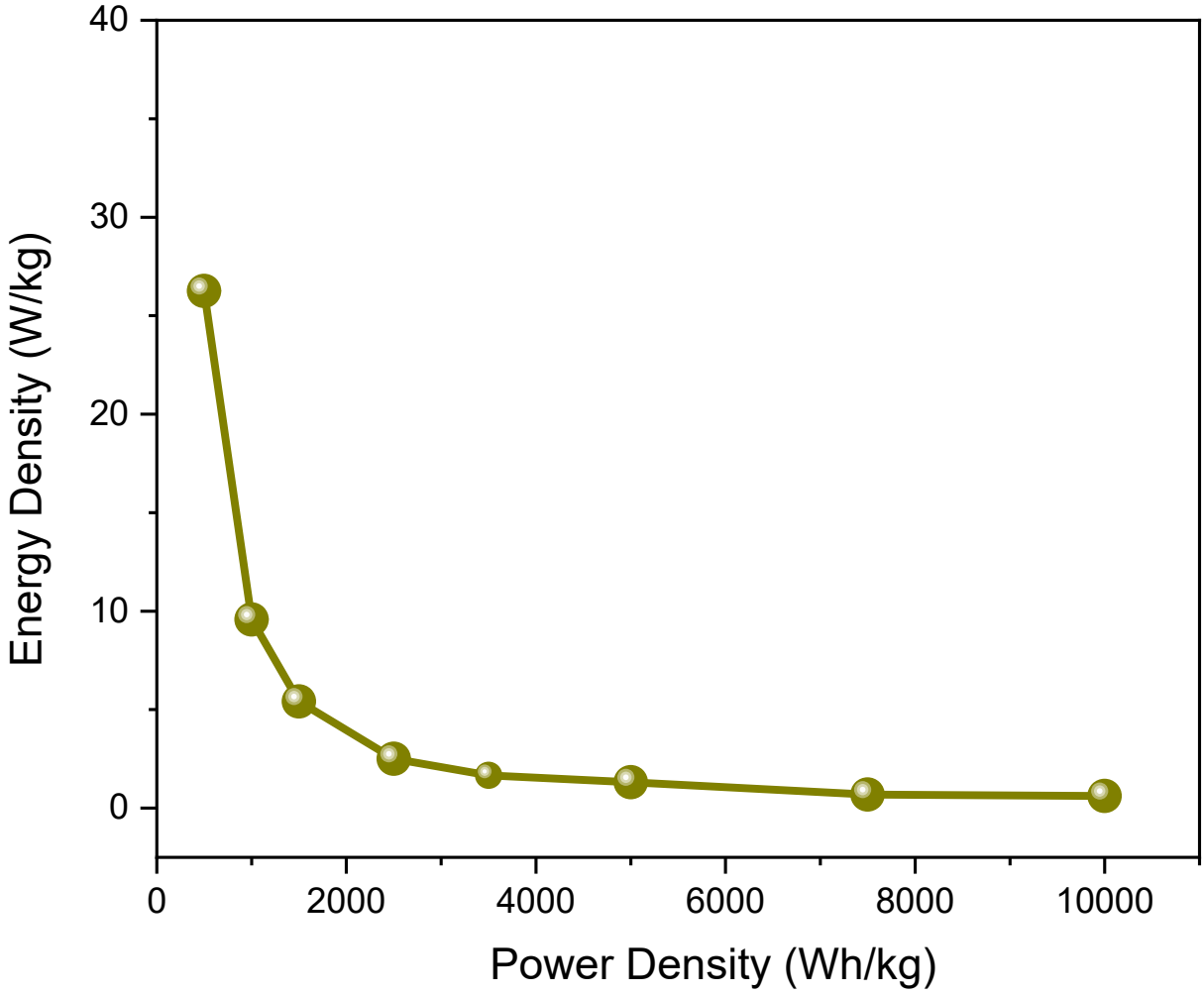


**Figure S5**. Ragone plots of CE-Py POP/SWCNT-AS (device) nanocomposite.

**Table S1.** Comparison the specific capacitance of CE-Py POP and CE-Py POP/SWCNT nanocomposite with those of previously reported materials for supercapacitor application.

| Electrode | Capacitance | Ref. |
|---|---|---|
| **CE-Py POP** | 122 F $g^{-1}$ at 0.5 A $g^{-1}$ | This work |
| **CE-Py POP/SWCNT** | 346 F $g^{-1}$ at 0.5 A $g^{-1}$ | This work |
| **Cz-Cz CMP** | 43.70 F $g^{-1}$ at 0.5 A $g^{-1}$ | **S1** |
| **Cz-TP CMP** | 67.38 F $g^{-1}$ at 1 A $g^{-1}$ | **S1** |
| **POSS-F-POIP** | 36.2 F $g^{-1}$ at 0.5 A $g^{-1}$ | **S2** |
| **H-THAQ** | 15 F $g^{-1}$ at 1 A $g^{-1}$ | **S3** |
| **THAQ/rGO (2:1)** | 76 F $g^{-1}$ at 1 A $g^{-1}$ | **S3** |
| **Pure AQ** | 42 F $g^{-1}$ at 1 A $g^{-1}$ | **S4** |
| **TPE-DDSQ-POIP** | 22 F $g^{-1}$ at 1 A $g^{-1}$ | **S5** |
| **Car-DDSQ-POIP** | 23 F $g^{-1}$ at 1 A $g^{-1}$ | **S5** |
| **OVS-A HPP** | 120 F $g^{-1}$ at 0.5 A $g^{-1}$ | **S6** |
| **OVS-P-A HPP** | 177 F $g^{-1}$ at 0.5 A $g^{-1}$ | **S6** |
| **Py-PDT POP** | 28 F $g^{-1}$ at 0.5 A $g^{-1}$ | **S7** |
| **TBN-BSU CMP** | 70 F $g^{-1}$ at 0.5 A $g^{-1}$ | **S8** |
| **Py-BSU CMP** | 38 F $g^{-1}$ at 0.5 A $g^{-1}$ | **S8** |
| **N- doped Porous carbons ropes** | 60 F $g^{-1}$ at 1.0 A $g^{-1}$ | **S8** |
| **TPE-FFC-CMP/CD-BZ** | 7.53 F $g^{-1}$ at 0.5 A $g^{-1}$ | **S9** |
| **TPE-FFC-CMP/poly (CD-BZ)** | 37.07 F $g^{-1}$ at 0.5 A $g^{-1}$ | **S9** |
| **Py-FFC-CMP/CD-BZ** | 10.15 F $g^{-1}$ at 0.5 A $g^{-1}$ | **S9** |
| **Py-FFC-CMP/poly (CD-BZ)** | 46 F $g^{-1}$ at 0.5 A $g^{-1}$ | **S9** |
| **HPC-0** | 48 F $g^{-1}$ at 1 A $g^{-1}$ | **S10** |
| **H-THAQ** | 15 F $g^{-1}$ at 1 A $g^{-1}$ | **S11** |
| **poly(TPA–DHTP–BZ) POP** | 67.1 F $g^{-1}$ at 0.5 A $g^{-1}$ | **S12** |
| **TPA-OXD-CMP/SWCNT** | 360 F $g^{-1}$ at 0.5 A $g^{-1}$ | **S13** |
| **TBN-TPE-CMP/SWCNT** | 156 F $g^{-1}$ at 0.5 A $g^{-1}$ | **S14** |

| | | |
|---|---|---|
| **TBN-Car-CMP/SWCNT** | 53 F $g^{-1}$ at 0.5 A $g^{-1}$ | **S14** |
| **CuTAPP-CMP/CNTs-1** | 70 F $g^{-1}$ at 1 A $g^{-1}$ | **S15** |
| **CuTAPP-CMP/CNTs-2** | 31 F $g^{-1}$ at 1 A $g^{-1}$ | **S15** |
| **CuTAPP-CMP/CNTs-3** | 207.8 F $g^{-1}$ at 1 A $g^{-1}$ | **S15** |
| **CuTAPP-CMP/CNTs-4** | 47.7 F $g^{-1}$ at 1 A $g^{-1}$ | **S15** |
| **CoCP/CNTs** | 31.5 F $g^{-1}$ at 1 A $g^{-1}$ | **S16** |
| **CoCP-CMP/CNTs** | 212 F $g^{-1}$ at 1 A $g^{-1}$ | **S16** |

| Sample | Rs (Ω) | Rct (Ω) | CPE-EDL ($S \cdot s^n$) | CPE-P ($S \cdot s^n$) |
|---|---|---|---|---|
| CE-Py POP | 6.54 | 26.30 | 0.0000605 | 0.000026 |
| CE-Py POP/SWCNT | 5.60 | 10.43 | 0.0000026 | 0.000078 |
| CE-Py POP/SWCNT-AS (device) | 39.13 | 76.80 | 0.00000006 | 0.00104 |

**Table S2.** Characteristics of Fitted Nyquist Plots of the POP-CMPs.

## References

[S1] S.F. Saber, S.U. Sharma, J.T. Lee, A.F.M. EL-Mahdy, S.W. Kuo, Carbazole-conjugated microporous polymers from Suzuki–Miyaura coupling for supercapacitors, Polymer 254 (2022) 125070. doi.org/10.1016/j.polymer.2022.125070.

[S2] M.G. Mohamed, T.H. Mansoure, Y. Takashi, M.M. Samy, T. Chen, S.W. Kuo, Ultrastable porous organic/inorganic polymers based on polyhedral oligomeric silsesquioxane (POSS) hybrids exhibiting high performance for thermal property and energy storage, Microporous Mesoporous Mater. 328 (2021) 111505. doi.org/10.1016/j.micromeso.2021.111505.

[S3] L. Xu, R. Shi, H. Li, C. Han, M. Wu, C.P. Wong, F. Kang, B. Li, Pseudocapacitive anthraquinone modified with reduced graphene oxide for flexible symmetric all-solid-state supercapacitors, Carbon 127 (2018) 459-468. doi.org/10.1016/j.carbon.2017.11.003.

[S4] B. Guo, Y. Yang, Z. Hu, Y. An, Q. Zhang, X. Yang, X. Wang, H. Wu, Redox-active organic molecules functionalized nitrogen-doped porous carbon derived from metal-organic framework as electrode materials for supercapacitor, Electrochim. Acta, 223 (2017) 74–84. doi.org/10.1016/j.electacta.2016.12.012.

[S5] M.G. Mohamed, W.C. Chen, A.F.M. EL-Mahdy, S.W. Kuo, Porous organic/inorganic polymers based on double-decker silsesquioxane for high-performance energy storage, J. Polym. Res. 28 (2021) 219. doi.org/10.1007/s10965-021-02579-x.

[S6] M. Ejaz, M.M. Samy, Y. Ye, S.W. Kuo, M.G. Mohamed, Design Hybrid Porous Organic/Inorganic Polymers Containing Polyhedral Oligomeric Silsesquioxane/Pyrene/Anthracene Moieties as a High-Performance Electrode for Supercapacitors, Int. J. Mol. Sci. 24 (2023) 2501. https://doi.org/10.3390/ijms24032501.

[S7] A.O. Mousa, M.G. Mohamed, C.H. Chuang, S.W. Kuo, Carbonized Aminal-Linked Porous Organic Polymers Containing Pyrene and Triazine Units for Gas Uptake and Energy Storage, Polymers 15 (2023) 1891. doi.org/10.3390/polym15081891.

[S8] M.G. Mohamed, S.Y. Chang, M. Ejaz, M.M. Samy, A.O. Mousa, S.W. Kuo, Design and Synthesis of Bisulfone-Linked Two-Dimensional Conjugated Microporous Polymers for $CO_2$ Adsorption and Energy Storage, Molecules 28 (2023) 3234. doi.org/10.3390/molecules28073234.

[S8] P. Thirukumaran, A. Parven, Y.R. Lee, S.C. Kim, Polybenzoxazine originated N-doped mesoporous carbon ropes as an electrode material for high-performance supercapacitors, J. Alloys Comp., 750 (2018) 384-391. doi.org/10.1016/j.jallcom.2018.04.034.

[S9] M.M. Samy, M.G. Mohamed, T.H. Mansoure, T.S. Meng, M.A.R. Khan, C.C. Liaw, S.W. Kuo, Solid state chemical transformations through ring-opening polymerization of ferrocene-based conjugated microporous polymers in host–guest complexes with benzoxazine-linked cyclodextrin, J. Taiwan Inst. Chem. Eng., 132 (2022) 104110. DOI: 10.1016/j.jtice.2021.10.010.

[S10] L. Wan, J. Wang, L. Xie, Y. Sun, K. Li, Nitrogen-enriched hierarchically porous carbons prepared from polybenzoxazine for high-performance supercapacitors, ACS Appl. Mater. Interfaces, 6 (2014) 15583–15596. DOI: 10.1021/am504564q.

[S11] L. Xu, R. Shi, H. Li, C. Han, M. Wu, C.P. Wong, F. Kang, B. Li, Pseudocapacitive anthraquinone modified with reduced graphene oxide for flexible symmetric all-solid-state supercapacitors, Carbon 127 (2018) 459-68. DOI: 10.1016/j.carbon.2017.11.003.

[S12] M. Ejaz, M.G. Mohamed, S.W. Kuo, Solid state chemical transformation provides a fully benzoxazine-linked porous organic polymer displaying enhanced $CO_2$ capture and supercapacitor performance. Polym. Chem., 14 (2023) 2494-2509. doi.org/10.1039/D3PY00158J.

[S13] M.G. Mohamed, M.M. Samy, T.H. Mansoure, S.U. Sharma, M.S. Tsai, J.H. Chen, J.T. Lee, S.W Kuo, Dispersions of 1,3,4-Oxadiazole-Linked Conjugated Microporous Polymers with Carbon Nanotubes as a High-Performance Electrode for Supercapacitors, ACS Appl. Energy Mater. 5 (2022) 3677–3688. https://doi.org/10.1021/acsaem.2c00100.

[S14] M.M. Samy, M.G. Mohamed, A.F.M. EL-Mahdy, T.H. Mansoure, K.C.W. Wu, S.W. Kuo, High-performance supercapacitor electrodes prepared from dispersions of tetrabenzonaphthalene-based conjugated microporous polymers and carbon nanotubes, ACS Appl. Mater. Interfaces 13 (2021) 51906-51916. https://doi.org/10.1021/acsami.1c05720.

[S15] L. Mei, J.C. Wei, Q. Duan, Construction of copper porphyrin-linked conjugated microporous polymer/carbon nanotube composite as flexible electrodes for supercapacitors. J. Mater. Sci. Mater. Electron. 32 (2021) 24953–24963. doi.org/10.1007/s10854-021-06952-w.

[S16] L. Mei, X. Cui, Q. Duan, Y. Li, X. Lv, H.G. Wang, Metal Phthalocyanine Linked Conjugated Microporous Polymer Hybridized with Carbon Nanotubes as a High-Performance Flexible Electrode for Supercapacitors. Int. J. Hydrogen Energy, 45 (2020) 22950-22958. doi.org/10.1016/j.ijhydene.2020.06.208.